Journal of Applied Polymer Science

Transformation of self-assembled structures from spherical aggregates in solution to a network structure on a two-dimensional surface

Xu Wu,[1] Jing Lin,[1] Danfeng Yu,[2] Jinben Wang,[2] Hui Yang,[2] Yuzhi Su,[1] Aiqing Ma,[3] Keji Sun,[3] Yibo Chen[1]

[1]College of Chemistry and Chemical Engineering, Guangzhou University, Guangzhou 510006, People's Republic of China
[2]Beijing National Laboratory for Molecular Sciences, Key Labratory of Colloid, Interface and Chemical Thermodynamics, Institute of Chemistry, Chinese Academy of Sciences, Beijing 100190, People's Republic of China
[3]Oil Production Technology Research Institute, Shengli Oilfield Branch Company, Sinopec, Dongying, Shandong 257000, People's Republic of China
Correspondence to: H. Yang (E-mail: yanghui@iccas.ac.cn)

ABSTRACT: Self-assembled films of brush-like amphiphilic copolymers with varying hydrophobic contents (fc_{12}, 10–90 mol %) were prepared on glass slides. In addition, the surface tension and contact angles of solutions of these copolymers were also investigated. By combining the data obtained investigating the morphologies of the films, with the micropolarities, dimensions, and morphologies of the copolymer aggregates in solution phase, it was attempted to illustrate how the self-assembled structures would adapt to a change in their surrounding environment from a three-dimensional space in the solution phase into a two-dimensional solid surface. The copolymer chains underwent inter- and intramolecular hydrophobic association simultaneously in the solution phase. When fc_{12} was increased, the stronger hydrophobicity led the side-chains that were attached to the same backbone to become packed together, and this intramolecular association caused the copolymers to form smaller and more compact spherical aggregates. The solutions of these smaller and more compact spherical aggregates exhibited a lower surface tension and better wetting behavior on glass surfaces. In addition, these solutions ultimately formed thinner and more orderly network-based porous films on glass surfaces. The observations described in this report revealed that the copolymer assemblies exhibited a morphological transformation from spherical aggregates in solution to a network structure when the copolymer became confined to a solid surface. © 2015 Wiley Periodicals, Inc. J. Appl. Polym. Sci. **2015**, *132*, 41945.

KEYWORDS: colloids; copolymers; morphology

Received 22 May 2014; accepted 28 November 2014
DOI: 10.1002/app.41945

INTRODUCTION

The self-assembly behavior of amphiphilic polymers either in solution or on solid surfaces is of significant scientific and technological importance due to their relevance to biomacromolecular systems and potential for various industrial applications.[1–6] Amphiphilic polymers incorporate hydrophilic and hydrophobic monomer units that are attached to the same polymer backbones,[7–9] and the self-assembly behavior of these polymers can be influenced by their inherent structures,[10,11] concentrations,[12,13] mixing ratios among multicomponent systems,[14,15] and external stimuli.[16,17] Generally, the self-assembled nanostructures of amphiphilic polymers can exhibit a wide range of architectural diversity, and these macromolecular nanostructures also tend to be more stable than the self-assembled structures of low molecular weight amphiphiles.[18,19]

In recent years, the development of surface modification techniques has led to the facile preparation of polymer films and facilitated the modification of surfaces.[20–29] However, the composition and homogeneity of these films were often poorly defined or differed from the expected composition. On solid supports, various kinds of macromolecular structures have been investigated, including those of linear block copolymers,[30,31] dendronized polymers,[32,33] special copolymers incorporating siloxane blocks,[21,34] or fluorinated units,[35,36] and composite polymer systems.[37,38] However, further fundamental studies are required in order to advance our understanding of the

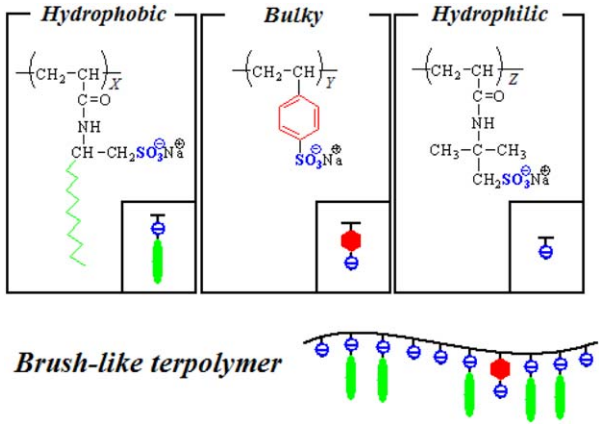

Figure 1. Illustration of the brush-like copolymer that incorporated hydrophobic ($AMC_{12}S$) units, bulky (SSS) units, and hydrophilic (AMPS) units. The subscripts in the structures shown above represent the mol % values for each unit, where $X = 10$, 30, 50, 70, and 90 mol %, $Y = 5$ mol %, and $Z = 95$ X mol %. [Color figure can be viewed in the online issue, which is available at wileyonlinelibrary.com.]

formation and structure of polymer films. Very little attention has been devoted to the changes that polymer aggregates undergo as they are transited from the solution phase and become confined onto a two-dimensional solid surface.

Our interest in amphiphilic polymers began almost a decade ago,[39,40] and a novel series of brush-like polymers with different side-chain compositions have been reported.[41–44] The polymers showed orderly self-assembly behavior in the solution phase, and this associative behavior was strongly dependent on the structures and the concentrations of the polymers. It was discovered for the first time that the presence of sterically bulky sodium *p*-styrenesulfonate (SSS) units on the copolymer backbone allowed the copolymer to retain its solubility in water, even when the content of the hydrophobic side-chains was increased up to 90 mol %. In addition, it was possible to investigate the influence of varying the mole fraction of the hydrophobic side-chains on the associative behavior of the amphiphilic copolymers.

The aggregates of the copolymers (Figure 1) in solution phase had been investigated by using steady-state fluorescence, dynamic light scattering (DLS), and transmission electron micrograph (TEM) in our previous work.[44] In the present work, the morphologies of the self-assembled films prepared from these copolymers with varying hydrophobic side-chain contents (ranging between 10 and 90 mol %) on solid supports were investigated. In addition to the morphologies of the copolymer films, the surface tension and contact angles of solutions of these copolymers were also investigated. By combining the morphologies and dimensions of the copolymer films observed on two-dimensional surfaces with the characteristics of the copolymer aggregates in solution, we attempted to gain an understanding of how the self-assembled structures adapted as their surroundings were changed from a solution phase to a two-dimensional surface. This work will provide valuable insight into the design and preparation of polymer films with well-defined functional nanostructures that exhibit tunable properties.

EXPERIMENTAL

Copolymers

The brush-like amphiphilic random terpolymers incorporating 2-(acrylamido)-dodecane sulfonic acid ($AMC_{12}S$, 10–90 mol %), sodium *p*-styrenesulfonate (SSS, 5 mol %), and 2-(acrylamido)-2-methylpropane-sulfonic acid (AMPS) units were synthesized, purified, and characterized according to the methods described in our previous report.[44] The copolymer compositions determined from the nitrogen-to-carbon ratios via elemental analysis were consistent with the feed ratios of the monomers prior to the polymerization, and the complete reactions of the monomers were determined by Solid-state ^{13}C NMR measurements.

Measurements

Sample Solution Preparation. Sample solutions for surface tension, contact angle measurements, and scanning electron microscopy (SEM) characterization were the same as that investigated in the previous work.[44] In a typical run, the solid copolymer samples were dissolved in water, and the solutions were heated to ~90°C and then continually stirred for another 15 min. After the solutions were cooled down to room temperature, the solutions were filtered with 0.45 μm membrane filters and stirred for 12 h prior to measurements.[45] The uncertainties in the copolymer concentrations are estimated to be less than or equal to $\pm(5 \times 10^{-4})$ g/L.

Film Preparation. Droplets of the copolymer solutions (1 g/L) were placed on glass slides and quickly frozen with liquid nitrogen.[46] Subsequently, they were freeze-dried under vacuum for seven days. The freeze-dried films on the glass surface were carefully moved to the sample stage and sputter-coated with palladium and gold prior to characterization.

Surface Tension Measurements. Surface tension curves of the copolymer solutions were obtained by using the drop-volume method at 25.0 ± 0.5°C.[47] A pendant droplet with ~90 vol % of a falling droplet was squeezed out of a capillary tip, and it was permitted to stand for an sufficient time to fall automatically to the surface below. The reported surface tension values were determined from at least five measured values, and the uncertainties are in the scope of $\pm$0.2 mN/m.

Contact Angle Measurements. The contact angles were measured via axisymmetric drop shape analysis (ADSA) at room temperature. Twenty microliter droplets of copolymer solutions (1 g/L) were created at the tip of a syringe and carefully placed onto the surfaces of glass slides. The contact angles were determined by analyzing the shapes of the droplets using a charge-coupled device (CCD) video camera and applying the Young-Laplace equation.[22]

Scanning Electron Microscopy. The morphologies of the assembled copolymer films that had been formed on glass surfaces were observed using a Hitachi S-530 scanning electron microscope.

Steady-State Fluorescence Measurement. The fluorescence experiments were conducted in our previous work.[44] The emission spectra were recorded on a Hitachi F-4500 spectrofluorometer at 25.0 ± 0.5°C. The measurements were carried out with the excitation at 335 nm and the slit widths at 2.5 nm. Pyrene was employed as the probe, and the concentration of pyrene in each sample solution was maintained to be 1×10^{-6} M.

Dynamic Light Scattering. DLS was carried out in the previous work using a LLS spectrometer (ALV/SP-125) with a multi-τ digital time correlater (ALV-5000).[44] Light ($\lambda = 632.8$ nm) from a solid-state He-Ne laser (22 mW) was used as the incident beam. The measurement was conducted at a scattering angle of 90°, 25.0 ± 0.1°C. The correlation function was analyzed with the CONTIN method.

Transmission Electron Micrograph. Morphology of the polymer aggregates in aqueous solution was characterized with a Hitachi H800 microscope in the previous work, and the direct magnification was of (1–8) × 10^4.[44] Negative staining (with uranyl acetate aqueous solution of 1 wt %) was used for TEM sample preparation.

RESULTS AND DISCUSSION

It was reported in a previous study that the presence of the bulky units would increase the maximum molar content of the hydrophobic $AMC_{12}S$ side-chains (fc_{12}) that the copolymer could possess while still retaining its solubility in water.[44] The retention of this solubility despite a dramatic increase of fc_{12} (up to 90 mol %) represents a new concept in the structural design of water soluble amphiphilic copolymers, and also led us to perform a systematic study on the influence of the hydrophobic side-chain content on the associative behavior. The associative behavior in the three-dimensional solution phase had been investigated by using steady-state fluorescence, DLS, and TEM in the previous work. It was discovered in this work that the structure of the copolymer aggregates in solution phase have a strong influence on the morphologies of the self-assembled films formed on two-dimensional surfaces. The inherent architectural correlations were observed between the morphologies of the films and those of the aggregates.

The copolymers adsorbed at the air/water interface would interact with the aggregates in the solution phase as the solvent evaporates during the formation of film on the solid surface. The surface tension of the copolymer solutions could provide information about the adsorption of polymer molecules at air/water interface. A plot of the variation of the surface tension versus the copolymer concentration is shown in Figure 2. The critical aggregation concentrations (CACs) of the copolymers determined from the clear breakpoints of the curves and the surface tension of 1 g/L copolymer solutions are listed in Table I. There is no clear breakpoint for the copolymers with $fc_{12} = 10$ mol % and $fc_{12} = 30$ mol %, which implies that the adsorption of these two copolymers keep changing along with the increase of concentrations. This also suggests that the associative behavior of the copolymers possessing less of the amphiphilic $AMC_{12}S$ side-chains could have a stronger tendency to change with the increase of concentrations, which is consistent with our previous results from the fluorescence and DLS. The CACs obtained from the surface tension breakpoints are larger than those obtained from the fluorescence spectroscopy analyses (Table I), although the values have the same decreasing tendency and the difference between the values tends to become relatively smaller when fc_{12} is increased. For example, the CAC determined by fluorescence for the

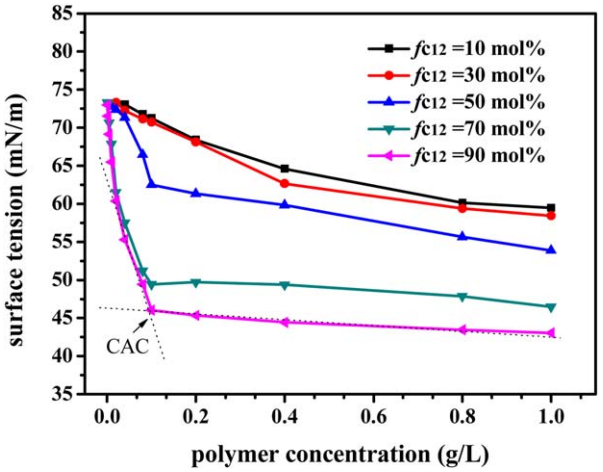

Figure 2. Plots of surface tension against the concentrations of copolymers with varying fc_{12} values ($fc_{12} = 10$, 30, 50, 70, and 90 mol %). [Color figure can be viewed in the online issue, which is available at wileyonlinelibrary.com.]

Table I. Contact Angles, Critical Aggregation Concentrations (CACs), and R_h of the Copolymers

Copolymer (fc_{12} mol %)	Surface tension (mN/m)[a]	Contact angle (°)[b]	CAC (g/kg)[c]	CAC (g/kg)[d]	R_h (nm)[e]
10	59.5	18.5	0.047	-	126.4
30	58.4	10.1	0.0074	-	26.9, 110.8
50	53.9	5.3	0.0039	0.11	20.4, 76.0
70	46.5	3.5	0.0027	0.094	38.5
90	43.0	2.4	0.0018	0.091	15.1

[a] The concentration of polymer solutions is 1 g/L.
[b] The concentration of polymer solutions is 1 g/L.
[c] Critical aggregation concentration determined by fluorescence spectroscopy analyses.
[d] Critical aggregation concentration determined by surface tension bending points.
[e] Apparent hydrodynamic radius determined by dynamic light scattering.

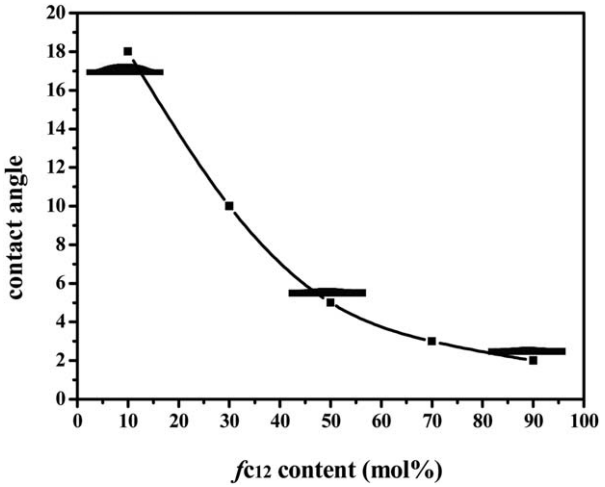

Figure 3. Measured contact angles exhibited by water droplets that had been placed on the surfaces of glass slides. These droplets contained 0.1 g/L of the copolymers, which had varying fc_{12} values (fc_{12} = 10, 30, 50, 70, and 90 mol %).

copolymers with fc_{12} = 90 mol % is 0.0018 g/kg, while that obtained from the surface tension versus is 0.091 g/kg. The obvious difference may be attributed to the twisting and entanglement of the polymer chains in solution phase rather than at air/water interface at the lower concentration. In other words, the copolymer may undergo aggregation at the concentration of 0.091 g/kg in solution phase while the adsorption at air/water interface is still in the process.

The surface tensions of the polymer solutions decreased when the polymer concentrations were increased, indicating the progressive adsorption of the polymer molecules at air/water interface along with the increase of concentrations. In addition, the surface tension of the copolymer solutions decreased when fc_{12} was increased, indicating that copolymers possessing more side-chains exhibited a lower surface tension. Generally, molecules that incorporate more amphiphilic units tend to exhibit a lower surface tension, such as gemini surfactants and trimeric surfactants,[47,48] since the chemical bond between the amphiphilic units in the same molecule would keep the units closer than those belonging to different single-chain molecules. Consequently, a more efficient adsorption and tighter arrangement may be formed at the air/water interface. However, the surface tension of the copolymers described in this report are in the range of 43–60 mN/m, which is obviously higher than that of small molecular surfactants, thus indicating that it would be relatively difficult for the copolymers to arrange in an orderly manner at the air/water interface. This difficulty may be caused by the hydrophobic interaction among the side-chains in the single copolymer molecule.

The measurements of contact angle were extensively used to study the compatibility of the films and specific solutions.[22,49] The wetting behavior of the copolymer solutions on a surface would also be a key factor that influences the thickness and structure of the polymer films. With this in mind, the contact angles of aqueous solutions of these copolymers were investigated on the surfaces of glass slides. Figure 3 shows the variation of the contact angles exhibited by droplets containing copolymers with varying fc_{12} values (10–90 mol %), and these values are also listed in Table I. The contact angles decreased with increases in fc_{12}, and the minimum contact angle observed for the copolymer with fc_{12} = 90 mol % was 2.4°. For the smooth glass surfaces, the contact angle is an equilibrium angle predicted by Young's equation.[50] It is logical that the polymer solution with a smaller liquid-vapor surface tension would has a lower contact angle, if the surface tensions at the solid-vapor and solid-liquid interfaces are assumed not change.[51] The copolymer solutions with lower contact angles would spread more readily over the surface, and thus had greater potential to form films with monolayer structures.

In Figure 4, the morphologies of the films prepared from copolymers with varying fc_{12} values are shown. Regardless of their varying molecular structures, it was apparent that all of the copolymers yielded porous network structures. In addition, the arrays of these mesh-like structures became progressively more continuous and orderly for the copolymers with higher fc_{12} values. The films also became thinner when they were prepared from copolymer solutions that exhibited lower contact angles, and films of the copolymer with fc_{12} = 90 mol % appeared to exhibit a monolayer structure [Figure 4(e)]. As mentioned earlier, this trend suggests that the thickness of the film is directly related to the contact angles of the copolymer solutions. The lower contact angle would lead to a relatively larger wetting scale, thus results in the less material on a volumetric basis and tends to be easier to form a film with monolayer structure. Because of their long range nanoporous structures, the network-based films observed here could have various potential applications, such as gas separation,[52] biosensors,[53] or catalyst supports.[54]

SEM images, TEM images, and R_h data for the self-assembled copolymer structures are shown in Figure 5, and the values of R_h are listed in Table I. The TEM images, R_h and the micropolarities of the copolymers in the solution phase were obtained in our previous work.[44] Besides the explanation according to Young's equation, the smaller aggregates for copolymer with greater fc_{12} may also contribute to the explanation of the lower contact angle. It is well known that the surface roughness or morphology could increase the contact angle.[53,54] The obvious size increase of the aggregates with hydrophilic surface may stick to and add rough characteristic to glass surface, and lead to the increase of contact angle. The morphologies of the structures observed both on the solid surfaces and in the solution phase could provide valuable information about how the structures adapt as they transit from a solvated state in solution to becoming confined on a solid surface. It can been seen in Figure 5(c,d) that the size of the spherical aggregates in the solution phase decreases from the scale of hundreds to that of tens of nm if fc_{12} is increased from 10 to 90 mol %. The broadening of the size distribution seen in Figure 5(f) over that seen in Figure 5(e) also supports this observation. There are several reasons to infer that the porous network structures are formed by the transformation or further assembly of the spherical aggregates. The spherical structures with about the same size as that in Figure 5(c) still could be observed in Figure 5(a). The spherical

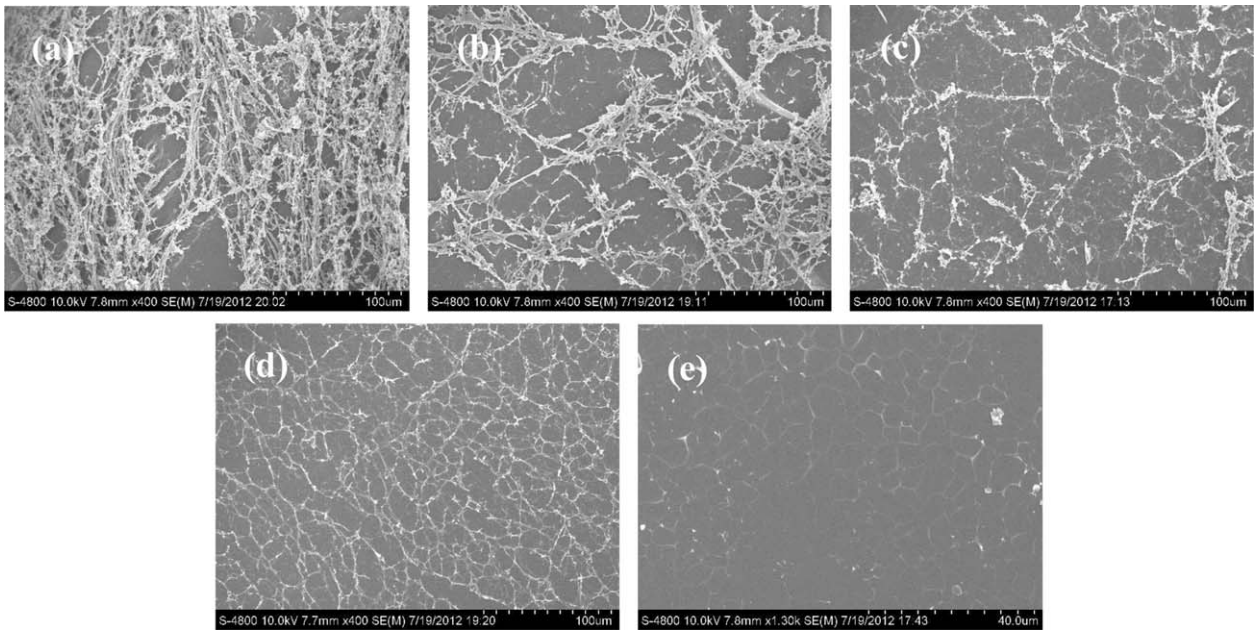

Figure 4. SEM images of copolymer films that had formed on the surfaces of glass slides. These films were composed of copolymers with various fc_{12} values including: fc_{12} = (a) 10, (b) 30, (c) 50, (d) 70, and (e) 90 mol %.

aggregates formed by the copolymer with $fc_{12} = 90$ mol % could be seen in both Figure 5(b,d), and the diameter of the cylinders in Figure 5(b) is comparable to the dimension of the separate spherical aggregates. The branching appears may because of growth defects,[55] which with linear cylinders together construct the network-based films. Theoretical prediction has shown that branching could occur in the one-dimensional aggregation of dipolar fluids when construction of a branch provides a lower free energy than the formation of a free chain end.[56] Images of the aggregates at different stages during the solvent evaporation would be indeed helpful for the further understanding of the structural transformation. However, only spherical aggregates were observed in the TEM images for the polymers with varying side chains and different concentrations. The different preparations of samples for TEM and SEM may interrupt the transition process of the aggregates, although the images could provide insight into the morphologies of the self-assembled structures in solution phase and on surface.

The micropolarities of the copolymer aggregates in the solution phase obtained from the fluorescence experiments were found to decrease dramatically with increases in fc_{12}, and this trend demonstrated that the aggregates became progressively more compact when the $AMC_{12}S$ side-chain content was increased. The loosely bound state of the aggregates of the copolymers with fewer $AMC_{12}S$ side-chains in the solution phase may account for the relatively irregular structure of the film observed in Figure 5(a). Meanwhile, copolymers with a greater fc_{12} value that form relatively compact aggregates in solution would be more likely to yield orderly network-based films, such as that observed in Figure 5(b).

On the basis of the experimental data both in solution phase and on surface aforementioned, the associative behavior of the copolymers was illustrated schematically in Figure 6. The copolymer chains undergo inter- and intramolecular hydrophobic associations simultaneously in the solution phase. When fc_{12} increases (10–90 mol %), the increase of the hydrophobicity promotes the side-chains in the same backbone to become packed together, and this preference for intramolecular association yields aggregates with smaller diameters and lower micropolarities. It is relatively difficult for the copolymers to be adsorbed efficiently and arrange in an orderly manner at air/water interface, which is most likely due to the intramolecular association. The copolymer solutions with the smaller and more compact spherical aggregates exhibited better wetting behavior on the surfaces of the glass slides, and thus formed thinner and more orderly network-based films composed of fused cylindrical assemblies.

An increase in the copolymer concentration would cause the copolymer to undergo a higher degree of intermolecular association between different polymer chains, and also promote further association between the aggregates, thus yielding larger aggregate structures. Therefore, the morphologies and sizes of the aggregates would be influenced by the copolymer concentration. This effect could also influence the structure and the size of the assemblies on solid surfaces. The transformation of the aggregates from a three-dimensional space in solution to a two-dimensional surface would cause the copolymer concentration to increase dramatically as the solvent evaporates. To offset this instability, a greater degree of association would occur between these aggregates and they would associate into larger structures in order to decrease their overall surface areas and increase the average density of hydrophilic groups that are exposed on their surfaces. Consequently, an adequate degree of solvent evaporation could trigger enhanced interactions between the spherical

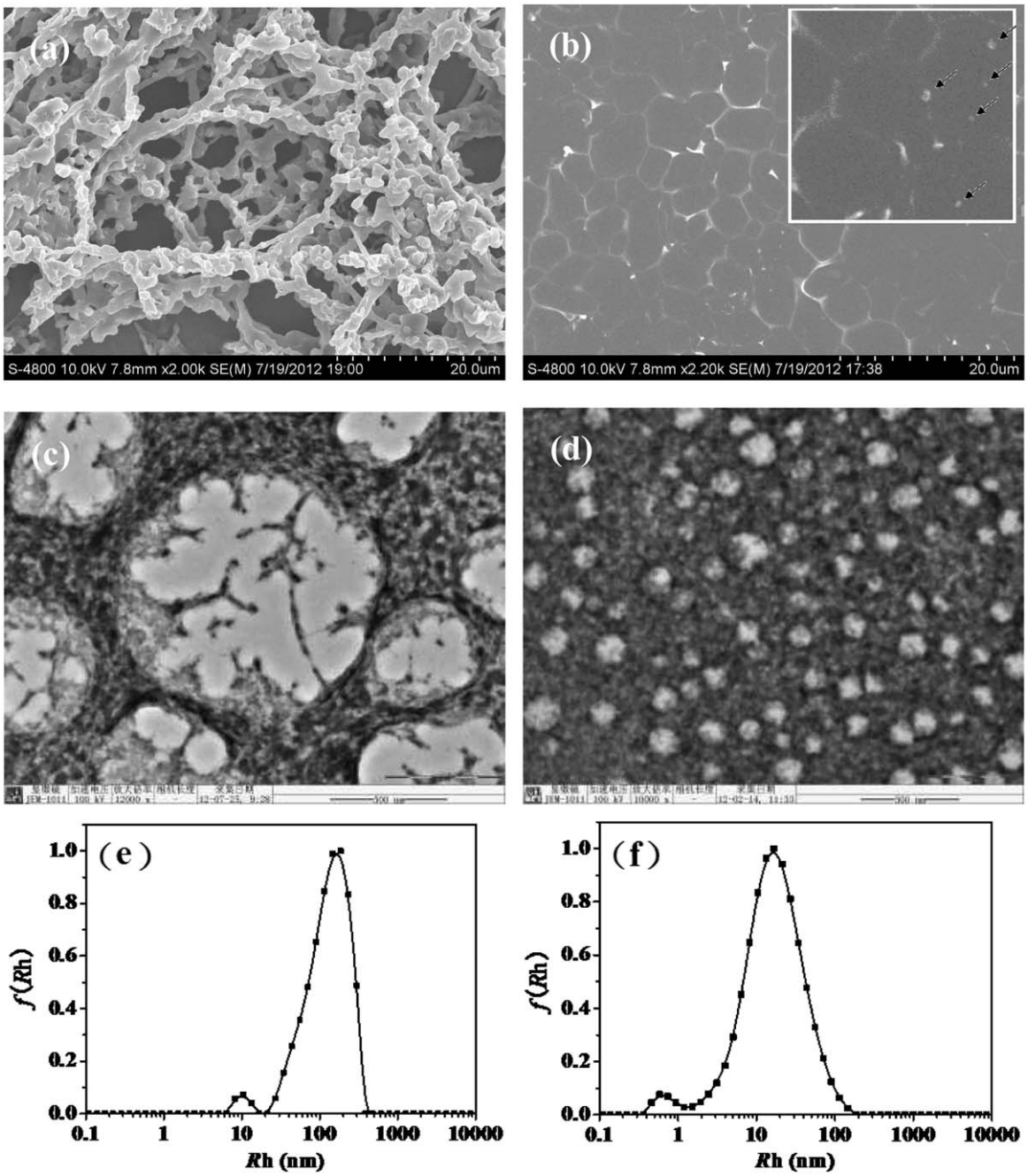

Figure 5. SEM images, TEM images, and R_h data of the self-assembled copolymer structures. Images (a) and (b) show SEM images of copolymers with $fc_{12} = 10$ and 90 mol %, respectively. Images (c) and (d) show TEM images of copolymers with $fc_{12} = 10$ and 90 mol %, respectively.[40] Images (e) and (f) show R_h of the copolymers with $fc_{12} = 10$ and 90 mol %, respectively.

copolymer aggregates, and these spherical aggregates could fuse together to yield cylindrical assemblies. These fused cylinders would subsequently provide the building blocks for the porous network-based films.

CONCLUSIONS

It was discovered in this work that the three dimensional aggregates of brush-like amphiphilic copolymers that were observed in solution became transformed into porous network structures when the copolymers became confined to two-dimensional surfaces. In addition, a correlation was observed between the aggregate structures observed in solution and the structures of the copolymer films that were observed on the surfaces. The copolymer chains simultaneously adopted inter- and intramolecular hydrophobic association in the solution phase. When the fc_{12} was increased (from 10 to 90 mol %) and the copolymer thus became more hydrophobic, the side-chains in the same backbone became more closely packed together, and the intramolecular association became favored. This close packing

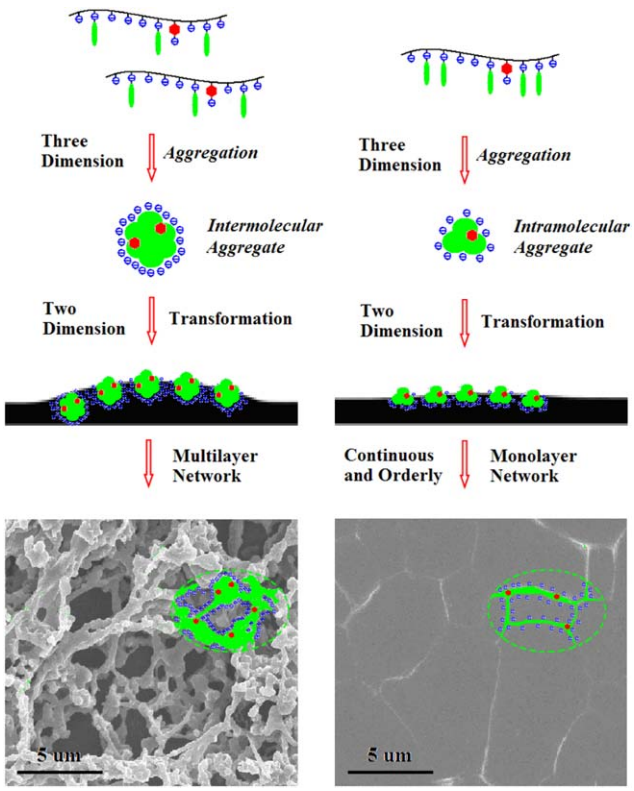

Figure 6. A schematic representation of the copolymer assemblies. The process observed at the left involved a copolymer with a lower fc_{12} value, while the process shown at the right involved a copolymer with a higher fc_{12} value. [Color figure can be viewed in the online issue, which is available at wileyonlinelibrary.com.]

yielded smaller and more compact spherical aggregates. The solutions of copolymers with higher fc_{12} values would have a lower surface tension, and the solutions of the copolymers described in this report had surface tension in the range of 43–60 mN/m. The surface tension was higher than those of small molecular surfactants, and demonstrated the difficulties encountered by the copolymers in forming highly ordered arrangements at the air/water interface due to the hydrophobic interaction among the side-chains in the single molecule. Droplets of copolymer solutions also exhibited lower contact angles on the surfaces of glass slides when fc_{12} was increased, and the lowest contact angle of 2.4° was observed for the copolymer with $fc_{12} = 90$ mol %. The spherical structures with about the same size could be seen in both the TEM and SEM results, and the diameter of the cylinders in the SEM image is comparable to the dimension of the separate spherical aggregates in the TEM image. The branching with linear cylinders together construct the network-based films. The solutions of copolymers with higher fc_{12} values formed thinner and more orderly network-based porous films covering the surfaces of glass slides. The transformation of the assembly structures from spherical aggregates in solution to network structures on solid surfaces may have been driven by the need for the copolymers to minimize their exposure to their surroundings as the copolymer concentration became too high for them to remain solvated because of the solvent evaporation.

ACKNOWLEDGMENTS

The authors are grateful to Ian Wyman, Department of Chemistry, Queen's University, for the revision of the manuscript. This work is financially supported by the National Natural Science Foundation of China (Grant Nos. 21406040, 51102054, and 21303026), and the Technology Project of Guangzhou (Grant No. 2013J4100023).

REFERENCES

1. McCormick, C. L. ACS Symposium Series 780; American Chemical Society: Washington, DC, **2001**.
2. Riess, G. *Prog. Polym. Sci.* **2003**, *28*, 1107.
3. Sambe, L.; Stoffelbach, F.; Lyskawa, J.; Delattre, F.; Fournier, D.; Bouteiller, L.; Charleux, B.; Cooke, G.; Woisel, P. *Macromolecules* **2011**, *44*, 6532.
4. Tanner, P.; Baumann, P.; Enea, R.; Onaca, O.; Palivan, C.; Meier, W. *Acc. Chem. Res.* **2011**, *44*, 1039.
5. Nottelet, B.; Patterer, M.; Francois, B.; Schott, M. A.; Domurada, M.; Garric, X.; Domurado, D.; Coudane, J. *Biomacromolecules* **2012**, *13*, 1544.
6. Dong, H.; Shu, J. Y.; Dube, N.; Ma, Y. F.; Tirrell, M. V.; Downing, K. H.; Xu, T. *J. Am. Chem. Soc.* **2012**, *134*, 11807.
7. Tomatsu, I.; Hashidzume, A.; Yusa, S.; Morishima, Y. *Macromolecules* **2005**, *38*, 7837.
8. Du, J. Z.; Chen, D. P.; Wang, Y. C.; Xiao, C. S.; Lu, Y. J.; Wang, J.; Zhang, G. Z. *Biomacromolecules* **2006**, *7*, 1898.
9. Feng, K.; Xie, N.; Chen, B.; Zhang, L. P.; Tung, C. H.; Wu, L. Z. *Macromolecules* **2012**, *45*, 5596.
10. Ueda, M.; Hashidzume, A.; Sato, T. *Macromolecules* **2011**, *44*, 2970.
11. Kawata, T.; Hashidzume, A.; Sato, T. *Macromolecules* **2007**, *40*, 1174.
12. Yamamoto, H.; Morishima, Y. *Macromolecules* **1999**, *32*, 7469.
13. Suwa, M.; Hashidzume, A.; Morishima, Y.; Nakato, T.; Tomida, M. *Macromolecules* **2000**, *33*, 7884.
14. Noda, T.; Hashidzume, A.; Morishima, Y. *Macromolecules* **2000**, *33*, 3694.
15. Noda, T.; Hashidzume, A.; Morishima, Y. *Macromolecules* **2001**, *34*, 1308.
16. Noda, T.; Hashidzume, A.; Morishima, Y. *Langmuir* **2000**, *16*, 5324.
17. Koh, H. D.; Changez, M.; Rahman, M. S.; Lee, J. S. *Langmuir* **2009**, *25*, 7188.
18. Moughton, A. O.; Hillmyer, M. A.; Lodge, T. P. *Macromolecules* **2012**, *45*, 2.
19. Rakhmatullina, E.; Braun, T.; Chami, M.; Malinova, V.; Meier, W. *Langmuir* **2007**, *23*, 12371.
20. Rabnawaz, M.; Liu, G. *J. Macromolecules* **2012**, *45*, 5586.
21. Bier, A. K.; Bognitzki, M.; Schmidt, A.; Greiner, A. *Macromolecules* **2012**, *45*, 633.
22. Jachimska, B.; Kozlowska, A.; Pajor-Swierzy, A. *Langmuir* **2012**, *28*, 11502.

23. Xiong, D.; Liu, G. J.; Duncan, E. J. S. *ACS Appl. Mater. Interfaces* **2012**, *4*, 2445.
24. Shi, Z. Q.; Wyman, I.; Liu, G. J.; Hu, H.; Zou, H. L.; Hu, J. W. *Polymer* **2013**, *54*, 6406.
25. He, G. P.; Hu, J. W.; Liu, G. J.; Li, Y. H.; Zhang, G. W.; Liu, F.; Sun, J. P.; Zou, H. L.; Tu, Y. Y.
26. Xiao, D. S. *ACS Appl. Mater. Interfaces* **2013**, *5*, 2378.
27. Ariga, K.; Yamauchi, Y.; Rydzek, G.; Ji, Q. M.; Yonamine, Y.; Wu, K. C. W.; Hill, J. P. *Chem. Lett.* **2014**, *43*, 36.
28. Li, Y. N.; Sonar, P.; Murphy, L.; Hong, W. *Energy Environ. Sci.* **2013**, *6*, 1684.
29. Yabu, H.; Higuchi, T.; Jinnai, H. *Soft Matter* **2014**, *10*, 2919.
30. Li, X.; Yu, X. H.; Han, Y. C. *Langmuir* **2012**, *28*, 10584.
31. Koh, K.; Liu, G. J.; Willson, C. C. *J. Am. Chem. Soc.* **2006**, *128*, 15921.
32. Chen, Y. B.; Ambade, A. V.; Vutukuri, D. R.; Thayumanavan, S.; Thayumanavan, S. *J. Am. Chem. Soc.* **2006**, *128*, 14760.
33. Shau, S. M.; Chang, C. C.; Lo, C. H.; Chen, Y. C.; Juang, T. Y.; Dai, S. A.; Lee, R. H.; Jeng, R. J. *ACS Appl. Mater. Interfaces* **2012**, *4*, 1897.
34. Khan, M. S. U.; Akhter, Z.; Iqbal, N.; Siddiq, M. *J. Organomet. Chem.* **2013**, *745*, 312.
35. Zou, H. L.; Lin, S. D.; Tu, Y. Y.; Liu, G. J.; Hu, J. W.; Li, F.; Miao, L.; Zhang, G. W.; Luo, H. S.; Liu, F.; Hou, C. M.; Hu, M. L. *J. Mater. Chem. A* **2013**, *1*, 11246.
36. Xiong, D.; Liu, G. J.; Hong, L. Z. *Chem. Mater.* **2011**, *23*, 4357.
37. Zhang, G. W.; Hu, J. W.; Liu, G. J.; Zou, H. L.; Tu, Y. Y.; Li, F.; Hu, S. Y.; Luo, H. S. *J. Mater. Chem. A* **2013**, *1*, 6226.
38. Xiong, D.; Liu, G. J. *Langmuir* **2012**, *28*, 6911.
39. Li, R. Q.; Wei, L. B.; Hu, C. C.; Xu, C. F.; Wang, J. B. *J. Phys. Chem. B* **2010**, *114*, 12448.
40. Zhang, P.; Zhang, L.; Zhang, L.; Zhou, J. Z.; Wang, J. B.; Yan, H. K. *J. Phys. Chem. B* **2012**, *116*, 12760.
41. Wu, X.; Qiao, Y. J.; Yang, H.; Wang, J. B. *J. Colloid Interface Sci.* **2010**, *349*, 560.
42. Wu, X.; Qiao, Y. J.; Wang, J. B. *J. Chem. Eng. Data* **2010**, *55*, 919.
43. Wu, X.; Wang, J. B.; Yang, H.; Shi, X. F. *Supramol. Chem.* **2013**, *25*, 151.
44. Wu, X.; Cai, X. X.; Hao, A. H.; Wang, J. B. *J. Chem. Eng. Data* **2013**, *58*, 927.
45. Yamamoto, H.; Tomatsu, I.; Hashidzume, A.; Morishima, Y. *Macromolecules* **2000**, *33*, 7852.
46. Zhao, Y. Z.; Zhou, J. Z.; Xu, X. H.; Liu, W. B.; Zhang, J. Y.; Fan, M. H.; Wang, J. B. *Colloid Polym. Sci.* **2009**, *287*, 237.
47. Wu, C. X.; Hou, Y. B.; Deng, M. L.; Huang, X.; Yu, D. F.; Xiang, J. F.; Liu, Y.; Li, Z. B.; Wang, Y. L. *Langmuir* **2010**, *26*, 7922.
48. Alami, E.; Holmberg, K.; Eastoe, J. *J. Colloid Interface Sci.* **2002**, *247*, 447.
49. Dutta, K.; Mahale, R. Y.; Arulkashmir, A.; Krishnamoorthy, K. *Langmuir* **2012**, *28*, 10097.
50. Young, T. *Philos. Trans. R. Soc.* **1805**, *95*, 65.
51. Bellanger, H.; Darmanin, T.; Givenchy, E. T.; Guittard, F. *Chem. Rev.* **2014**, *114*, 2694.
52. Wu, L. B.; An, D.; Dong, J.; Zhang, Z. M.; Li, B. G.; Zhu, S. P. *Macromol. Rapid Commun.* **2006**, *27*, 1949.
53. Bayley, H.; Cremer, P. S. *Nature* **2001**, *413*, 226.
54. Schüth, F.; Sing, K. S. W.; Weitkamp, J. Handbook of Porous Solids, Wiley-VCH: Weinheim, **2002**.
55. Cui, H. G.; Chen, Z. Y.; Zhong, S.; Wooley, K. L.; Pochan, D. J. *Science* **2007**, *317*, 647.
56. Tlusty, T; Safran, S. A. *Science* **2000**, *290*, 1328.